Magnetic circular dichroism and the optical detection of magnetic resonance for the Bi antisite defect in $Bi_{12}GeO_{20}$

1995 J. Phys.: Condens. Matter 7 6951

(http://iopscience.iop.org/0953-8984/7/34/017)

J. Phys.: Condens. Matter 7 (1995) 6951–6959. Printed in the UK

Magnetic circular dichroism and the optical detection of magnetic resonance for the Bi antisite defect in $Bi_{12}GeO_{20}$

B Briat†, H J Reyher‡, A Hamri†, N G Romanov†‖, J C Launay§ and F Ramaz†

† Laboratoire d'Optique Physique, ESPCI, 10 rue Vauquelin, 75231 Paris Cédex 05, France
‡ Fachbereich Physik, Universität Osnabrück, 49069 Osnabrück, Germany
§ Laboratoire de Chimie du Solide, Université de Bordeaux 1, 22405, Talence Cédex, France

Received 24 March 1995, in final form 24 May 1995

Abstract. We report on the optical detection of electron paramagnetic resonance at 36 GHz, 67 GHz and 70 GHz for all the absorption bands of $Bi_{12}GeO_{20}$ (BGO) in the visible spectral range. This completes our previous studies and demonstrates clearly that the three major magnetic circular dichroism features do belong to the same isotropic centre, i.e., a $Bi^{3+}_{Ge} + h$ defect with the hole being delocalized onto the four surrounding oxygen atoms. We provide a simple explanation for the unusual sign of ODMR and the transient behaviour of the magnetic circular dichroism at resonance.

1. Introduction

The presence of point defects or doping ions in the crystal structure of bismuth sillenites $Bi_{12}MO_{20}$ (BSO, BGO and BTO for M=Si, Ge, Ti) is a prerequisite for the generation and transfer of photoinduced charge carriers that are responsible for photochromic and photorefractive phenomena in these technologically important materials [1]. It has long been suggested [2–5] that an intrinsic defect plays an important role in these crystals, since the photorefractive effect is observed even in nominally undoped crystals. Magnetic circular dichroism (MCD) provided the first demonstration [6, 7] that a paramagnetic centre is indeed present in as-received undoped crystals. It then developed [8, 9] that this centre, which is not present in thermally bleached (600 °C in the dark) samples, is created by blue illumination at relatively low temperatures. A similar conclusion was reached from optical absorption measurements [10, 11]. More recently, two of the present authors have detected optically the electron paramagnetic resonance of the centre [12, 13]. The theoretical interpretation of the observed positive g shift, of the relatively small hyperfine coupling constant A, and of the isotropy of these quantities led to the picture of a highly covalent defect, which consists of a hole mainly located on the four oxygen neighbours of a tetrahedrally coordinated Bi^{3+} ion.

For technical reasons (crystal thickness, nature of the detector), these optically detected magnetic resonance (ODMR) measurements were restricted to energies below 19 000 cm^{-1}. Furthermore, some of the crystals investigated contained aluminium and chromium [13] which eventually introduce their own related paramagnetic centres [6]. Additional ODMR results have now been obtained for nominally pure BGO in our two laboratories, with

‖ Permanent address: A F Ioffe Physico-Technical Institute, 194021 Saint Petersburg, Russia.

0953-8984/95/346951+09$19.50

crystals of an appropriate thickness (about 0.6 mm) to cover the higher-energy region. Their discussion is the object of the present paper.

2. Experimental details

MCD ($\Delta\alpha$ in cm^{-1}) is the differential absorption for left (σ_+) and right (σ_-) circularly polarized lights, induced by a magnetic field B which is applied along the direction of propagation k of the beam. We apply the chemist's convention to define 'right', i.e., an observer receiving the radiation observes a clockwise rotation of the electric vector tip in a plane perpendicular to k.

Our instruments and their calibration have been described elsewhere [14, 15]. ODMR was measured by monitoring MCD at helium temperatures and at microwave frequencies of 36 GHz (klystron, 500 mW), 70 GHz (Gunn diode, 100 mW) and 67 GHz (klystron, 100 mW). No cavity was used, the crystals simply being fixed below the end of the vertical 35 GHz waveguide leading into the cryostat. Besides the EPR transitions with $\Delta M_s = \pm 1$ which are allowed for the $S_\pm$ operator (relevant for a transversal B_1 oscillating magnetic field), we could see transitions with $\Delta M_s = 0$ (S_z appropriate for longitudinal B_1).

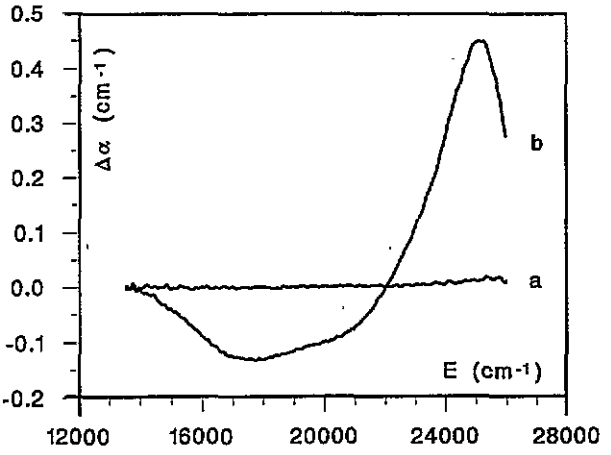

Figure 1. The MCD spectrum ($\Delta\alpha$ in cm^{-1}) of BGO in the visible spectral region under 2.5 T. The sample has been thermally bleached at 600 °C, then cooled down to 4.2 K (spectrum a) and subsequently coloured by illumination at 22 000 cm^{-1} (spectrum b).

3. Results

Figure 1 illustrates the MCD of BGO at 4.2 K under a field of 2.5 T in two extreme situations. In the thermally bleached state (figure 1, spectrum a), the signal is essentially zero, this demonstrating that no paramagnetic centre contributes in the visible–near-UV spectral region. By contrast, a subsequent blue illumination of the sample leads to two negative features at 17 600 cm^{-1} and around 20 500 cm^{-1} and one strong positive one at 25 000 cm^{-1}. All three features have counterparts in the optical absorption spectrum [10, 11] of coloured crystals.

The three MCD bands are temperature dependent and correspond therefore to one or several paramagnetic centres. Furthermore, their field variation at 1.4 K was shown to

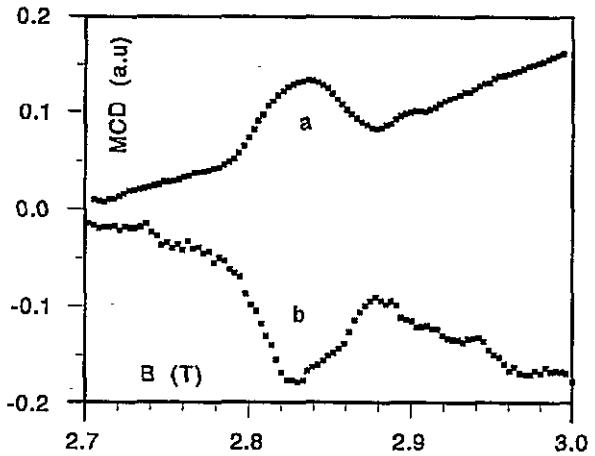

Figure 2. The ODMR of BGO at 36.2 GHz, recorded by monitoring the MCD, with the monochromator set at 24 500 cm^{-1} (a) and 17 600 cm^{-1} (b). In each instance, the value at thermal equilibrium for $B = 2.7$ T was subtracted and an appropriate straight 'base line' was subtracted to magnify the resonance. $T = 1.5$ K; $\boldsymbol{B} \parallel [110]$.

follow a Langevin function for a spin $\frac{1}{2}$ with a g factor close to two, under the condition that a sufficient amount of time (e.g., 5 min) is waited at each magnetic field value to reach thermal equilibrium.

Figure 2 shows our ODMR signals at 36.2 GHz, for $\boldsymbol{B} \parallel [110]$, with the monochromator set at 24 500 cm^{-1} (a) or 17 600 cm^{-1} (b). The resonance field is clearly the same (2.83 T) for the two peaks. We underline the fact that |MCD| increases (we shall subsequently refer to $\Delta|\text{MCD}| > 0$ in this situation) at resonance (by roughly 2%) while a decrease is usually observed in a 'normal' ODMR experiment [16]. The two curves shown in figure 2 were taken with a step of 3 mT and a time constant τ of 0.4 s at the lock-in by first raising the field rather quickly (0.2 s) to a given value, waiting 3τ s and then accumulating 200 data points during 8 s and averaging (roughly 16 min for a record).

As shown in figure 3, ODMR results at 70 GHz ($\boldsymbol{B} \parallel [110]$) exhibit a large number of resonances. The sampling conditions were somewhat faster than the above ones and the microwave-induced MCD change is here of the order of 10%. Again, the results are essentially similar for the negative and positive MCD peaks. We note however that, although $\Delta|\text{MCD}|$ is positive for the three major resonances (1–3), the sign is opposite for ODMR signal 4. A number of additional features (double-quantum transitions corresponding to EPR at 2×70 GHz) which were clearly seen in our previous experiment on BTO [13] show up as weak signals in the 2–3 T range.

Finally, at 67 GHz (figure 4), two resonances were observed (for the two bands), one at 1.20 and one at 1.51 T, for $\boldsymbol{B}$ directed along [100] as well as for $\boldsymbol{B}$ along [110]. The Nd^{3+} dopant which sits at the Bi site does not play a role here.

It is well established [16] that MCD tagged by EPR (tagged MCD) can be useful to complement ODMR experiments. In this case, the magnetic field is set at resonance and the microwave-induced change of MCD is measured as a function of the wavenumber and then scaled to be compared to the MCD. In figure 5, the remarkable coincidence of the two spectra confirms that the three MCD features shown in figure 1 do belong to only one centre.

We have observed previously [8, 12] that the spin temperature can be significantly

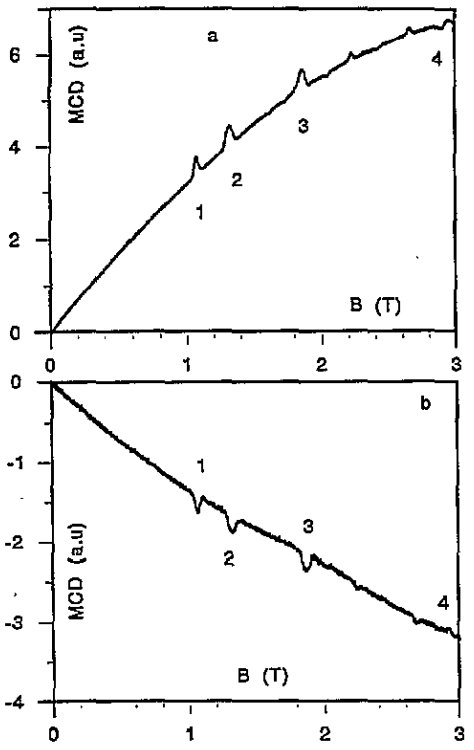

Figure 3. The ODMR of BGO at 70 GHz with the monochromator set at 25 000 cm^{-1} (a) and 16 700 cm^{-1} (b). The CD value in zero field was subtracted. The ordinate unit is arbitrary but the same for the two spectra. EPR transitions are marked by 1–4. Other resonances belong to double-quantum transitions. T = 1.6 K; $B \parallel [110]$.

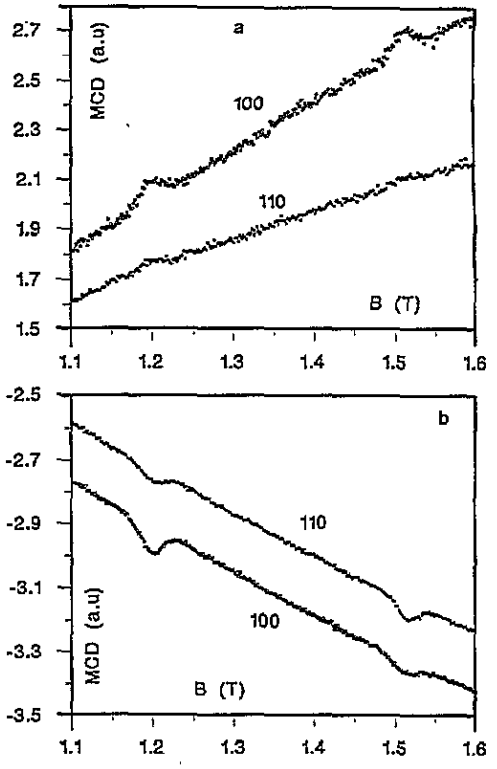

Figure 4. The ODMR of BGO:Nd at 67 GHz (1.4 K) with the monochromator set at 23 000 cm^{-1} (a) and 17 600 cm^{-1} (b). Experiments have been carried out on two crystals cut perpendicular to [110] and [100] respectively.

different from the bath temperature in the case of sillenite crystals. This is observed as a delay [8] for the establishment of the equilibrium MCD after a change of magnetic field, or when a resonant microwave field is switched on or off. Figure 6 illustrates this point beautifully in the case of $Bi_{12}TiO_{20}$. The monochromator is set at 16 600 cm^{-1}, i.e., on the negative part of the MCD spectrum (see figure 1). After the stabilization of the MCD signal at 2.85 T (the first 180 s), the microwaves are switched on and there is a sudden rise of |MCD| for about 3 s, which is immediately followed by a very slow (44 s time constant) but large decrease until a final value (about 400 s), which is well below that at thermal equilibrium, is reached. The following drift (up to 600 s) results from a partial bleaching of the crystal with the monochromator light. An additional sharp decrease occurs when the microwaves are switched off. It is followed now by a slow but large increase of |MCD| until we reach Boltzmann equilibrium. The final value is of course smaller than the initial one because of the bleaching.

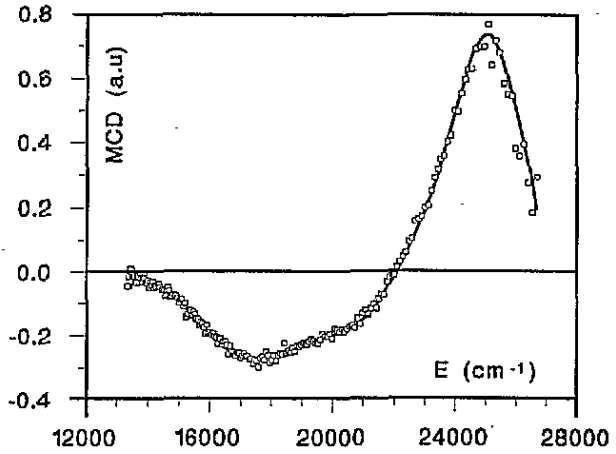

Figure 5. A comparison between the MCD spectrum of BGO in the absence of microwaves (full line) and the tagged MCD (open squares) for 1.075 T and 70 GHz. As compared to figure 1, the high-energy broad band is underestimated here, because of the uncorrected dark current becoming relevant in this region of low transmission (Osnabrück).

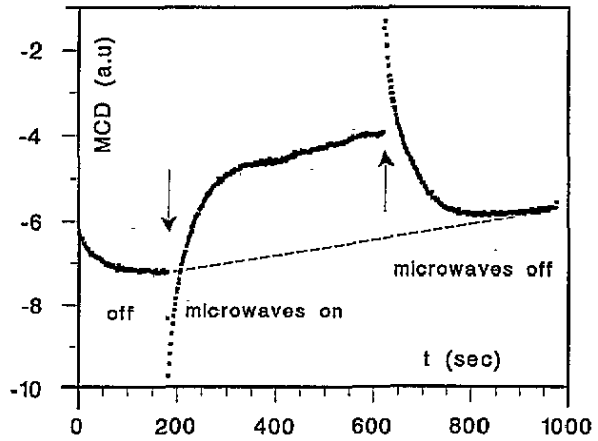

Figure 6. The response of the MCD for an aluminium-doped (5%) $Bi_{12}TiO_{20}$ crystal (transition $|4,-4\rangle \rightarrow |5,-5\rangle$) to the application of 36.2 GHz microwaves at resonance (2.85 T) of Bi^{4+}. The drift of the equilibrium MCD due to optical bleaching is shown by the dashed line.

4. Discussion

The most important result of this investigation is of course that all three major features of the MCD of BGO in the visible spectral range do belong to the same centre. Furthermore, our experiments with the external magnetic field directed along two orientations lead to the conclusion that the ODMR signals are isotropic. As will be seen below, we confirm therefore, by two independent sets of experiments, the nature of the defect as $Bi^{3+}_{Ge} + h$, as first proposed by Oberschmid and Grabmaier [4, 17] and demonstrated in our previous ODMR work [12, 13]. We refer to the latter for the basic arguments and rather address here in more detail the problem of the shape and sign of the observed ODMR features as well as the understanding of our kinetic results.

Let us just recall that we use an isotropic spin Hamiltonian

$$H = g\beta \boldsymbol{B}\cdot\boldsymbol{S} - g_n\beta_n \boldsymbol{B}\cdot\boldsymbol{I} + A\boldsymbol{I}\cdot\boldsymbol{S}. \tag{1}$$

The first two terms represent the electronic ($S = \frac{1}{2}$ for a hole) and the nuclear ($I = \frac{9}{2}$ for ^{109}Bi) Zeeman energies, respectively, and the third term accounts for the hyperfine interaction. Although the eigenvalues can simply be described by the Breit–Rabi formula [12], we also need the eigenvectors for further use. The total angular momentum of the system is $F = 4$ (lowest states) or $F = 5$. We refer to $|F, M\rangle$ for the individual Zeeman components with energy $E(F, M)$ and call $N(F, M)$ the associated normalized populations.

With $x = g_n\beta_n B/2$ and $y = g\beta B/2$, and using $|u\rangle = |M - \frac{1}{2}, +\frac{1}{2}\rangle$ and $|v\rangle = |M + \frac{1}{2}, -\frac{1}{2}\rangle$ as the $|M_I, M_s\rangle$ basis vectors, then for $|M| \leqslant 4$, the diagonal elements of the 2×2 matrices are

$$H_{uu} = (A/2)(M - \tfrac{1}{2}) - 2x(M - \tfrac{1}{2}) + y \qquad H_{vv} = -(A/2)(M + \tfrac{1}{2}) - 2x(M + \tfrac{1}{2}) - y$$

while the off-diagonal matrix element is $H_{uv} = (A/2)[(5 + M)(5 - M)]^{1/2}$. In the case where M is $+5$ or -5, the eigenvector (or eigenvalue) is simply $|u\rangle(H_{uu})$ or $|v\rangle(H_{vv})$.

For a given M, the eigenvectors have therefore the following general form:

$$|4, M\rangle = a_M|u\rangle + b_M|v \tag{2}$$

$$|5, M\rangle = -b_M|u\rangle + a_M|v\rangle. \tag{3}$$

The calculation of the MCD then proceeds as follows [18]:

$$\Delta\alpha \propto \sum N(4, M) \sum\{|\langle f|r_+|4, M\rangle|^2 - |\langle f|r_-|4, M\rangle|^2\} + \text{similar term for } F = 5 \tag{4}$$

where $r_\pm = (1/\sqrt{2})(r_x \pm \mathrm{i}r_y)$ stands for the electric pole moment operator. Although the actual composition of the excited states $|f\rangle$ is not known, one is allowed to replace $|f\rangle$ by the product $|j\rangle|M_I\rangle$ when calculating the sums $\sum|\langle f|r_\pm|4, M\rangle|^2$. j stands here for all quantum numbers of $|f\rangle$ except M_I. Since the hyperfine splitting in the excited state is surely small compared to the optical band width, the sum over the excited states includes all the $|M_I\rangle$. Then it is straightforward to obtain the following for $\Delta\alpha$:

$$\Delta\alpha = D[N(5, -5) - N(5, 5)] + D\sum[N(4, M) - N(5, M)][b_M^2 - a_M^2]. \tag{5}$$

D is the overall difference between the total cross sections for σ_+ and σ_- circularly polarized lights from the $M_s = -\frac{1}{2}$ electronic state ($D < 0$ at 17 600 cm^{-1}, cf. figure 1, spectrum b). The summation extends from $M = -4$ to $M = +4$.

In our experiments, resonance occurs for $\Delta M = M' - M = \pm 1 (S_\pm)$ or $\Delta M = 0 (S_z)$ when the distance ΔE (in gigahertz) between states of the type (3) and (2) is equal to the employed microwave frequency. Figure 7 shows an illustrative plot of ΔE versus the magnetic field, as calculated with the parameters $g = 2.041$ and $A = 19.21$ GHz which we have determined previously for BGO. This plot allows the assignment of the ODMR lines detected at both 70 (1–4) and 36 Ghz (1′). It explains also why the change of the microwave frequency from 70 to 67 GHz results in only two resonances since we are now below the bottom of the upper parabola.

For $-4 \leqslant M \leqslant 3$, the transitions $|4, M\rangle \rightarrow |5, M + 1\rangle$ and $|4, M + 1 \rightarrow |5, M\rangle$ are almost degenerate, with a positive splitting $2g_n\beta_n B$ between the latter ($\Delta M = -1$) and the former ($\Delta M = +1$). In view of figure 7, it is clear that the $\Delta M = -1$ transition is expected at a higher field than the $\Delta M = +1$ transition if we are on the descending part (left-hand side) of the approximate parabola representing ΔE versus B. The reverse situation is of course expected on the ascending part (right-hand side). (2) and (3) can be used to determine the transition probability R of EPR transitions ($\Delta M_I = 0$) with $R = (bb')^2$ when $\Delta M = +1$

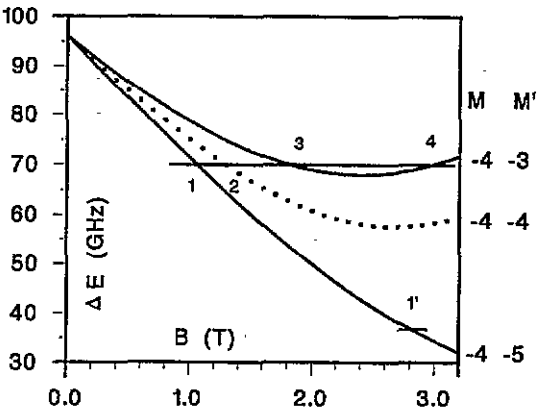

Figure 7. The calculated energy difference between the levels $|5, M'\rangle$ and $|4, M\rangle$ of Bi^{4+} in BGO ($g = 2.041$ and $A = 19.21$ GHz) and identification of the EPR transitions at 70 GHz (marked 1–4) and 36.2 GHz (1′). As explained in the text, the $|4, -4\rangle \rightarrow |5, -3\rangle$ and $|4, -3\rangle \rightarrow |5, -4\rangle$ transitions are almost degenerate and only that with $\Delta M = +1$ is shown here.

and $R = (aa')^2$ when $\Delta M = -1$. R is proportional to $2(ab)^2$ when $\Delta M = 0$ (we do not know precisely how much of the electromagnetic field is polarized along the z axis).

We have argued previously [12] that the system $Bi^{3+}+h$ is somewhat peculiar since one has two very different relaxation times: relatively fast relaxation (of the order of seconds) for $\Delta F = 1$, $\Delta M = 0, \pm 1$ (no nuclear spin flip) and slow relaxation (minutes) for $\Delta F = 0$, $\Delta M = \pm 1$ (nuclear spin flip). This has very important consequences for the rate of the build-up and decay of the ODMR signals as we shall shown now by interpreting figure 6. We consider the $|4, -4\rangle \rightarrow |5, -5\rangle$ transition because there is only one fast $\Delta F = 1$ relaxation working against the microwaves in this particular case. When we switch on the microwaves, the first step is that the population of the lowest state will decrease by ΔN (positive value) while that of the upper one will increase by the same amount. According to (5), the change of |MCD| will be $-\Delta N(b^2 - a^2) + \Delta N = 2\Delta N a^2$ (increase). The argument of course holds for any value of the magnetic field. In the second step, due to the slow relaxation process, a new 'thermal equilibrium' starts to develop. The populations $N(4, M)$ of all the levels located below $|4, -4\rangle$ decreases while those ($N(5, M)$) of the levels located above $|5, -5\rangle$ will increase. (5) then tells us that the overall |MCD| will decrease if the factors $b^2 - a^2$ are positive. We checked that this is indeed the case for $B \geqslant 2.7$ T. When we switch the microwaves off, we decrease $N(5-5)$ by ΔN and increase $N(4, -4)$ by the same amount. The net change is therefore $-\Delta N + \Delta N(b^2 - a^2) = -2\Delta N a^2$, i.e., a further decrease of |MCD|. Finally, we return to thermal equilibrium when $N(4, M)$ increases while $N(5, M)$ decreases.

Figure 6 shows that the opposite signs of ODMR may be observed depending on the time which is used to scan over the resonance line. Since we are dealing with inhomogenously broadened lines, one must compare the time during which a certain spin packet is at resonance with the time needed to obtain equilibrium conditions. Assuming some hundreds of spin packets per resonance curve and a typical time of 5 min for B being within a line in, e.g., figure 3, we may estimate that the individual spin packet undergoes transitions for a few seconds. From figure 6, we see that this means that we only observe the transient part of the microwave-induced change of the MCD. In this case a simple explanation can be given for the observed signs of the ODMR signals. We assume that a significant amount of population ΔN is transferred from the lower to the upper state when switching on

the microwave. Before the new equilibrium develops, it is straightforward to infer that the absolute value of the MCD will change by an amount $\Delta|\mathrm{MCD}| = \Delta N[(a^2-b^2)+(a'^2-b'^2)]$, where a, b and a', b' are from the levels in resonance. Our numerical calculations indeed predict that, in excellent agreement with the results presented in figures 2 and 3, $\Delta|\mathrm{MCD}|$ is positive for all the allowed lines, except for that around 3 T at 70 GHz. The same sign is predicted for the $|4,-4\rangle \rightarrow |5,-3\rangle$ and $|4,-3\rangle \rightarrow |5,-4\rangle$ transitions.

It is interesting to note that the above very simple arguments also explain the reversal of sign observed in the MCD–ESR work of Kunzer *et al* [19] for the Bi^{+}_{Ga} heteroantisite defect in GaAs. For the $|4,-4\rangle \rightarrow |5,-5\rangle$ transition at 1.63 T, one finds $\Delta|\mathrm{MCD}| = \Delta N[(a^2-b^2)+1] = 2\Delta N a^2$ (positive) while for the $|5,-5\rangle \rightarrow |5,-4\rangle$ transition at 2.06 T, $\Delta|\mathrm{MCD}| = \Delta N[(a^2-b^2)-1] = -2\Delta N b^2$ (negative).

For a very slow passage of the resonance line, the effects due to the relaxation of the whole hyperfine level system should become important. The general case of any transition at an arbitrary rate (microwave power) and at any field can only be described by rate equations. This seems to be an infeasible task because all the various relaxation processes possess different, field-dependent, rates. Nevertheless, one can understand some qualitative features which arise, if relaxation processes determine the ODMR line shapes for slow scan speeds. In [12], we found that all the degenerate transitions showed a derivative-like shape at 90 GHz, with a decrease of |MCD| at low field. These features are only faintly visible for the corresponding transitions in figure 3 (1.87 T and 2.92 T), due to the fast scans applied there. Integrating the arguments based on (5) into the 'microwave pumping' scheme developed in [12] we may assume that the population ΔN transferred to an upper M' state served essentially ($\Delta N'$) to populate the three lower $M = M'$, $M' \pm 1$ states ($\Delta N'/3$ to each, $\Delta N'$ close to ΔN). Using our $b^2 - a^2$ values at various field strengths we made estimates of $\Delta|\mathrm{MCD}|$ for the various transitions and found an excellent sign agreement with the previously observed features [12].

Finally, the signs of $\Delta|\mathrm{MCD}|$ shown in [13] for BTO:Al, Cr at 70 GHz and 700 nm are different from those observed in the present work. This was actually caused by the presence of chromium which has a strong positive MCD superimposed onto a weak negative one for the hole centre. Therefore, a rise of |MCD| for the latter results in a decrease of the total positive signal.

5. Conclusions

In summary, the three absorption and MCD features observed for BGO in the visible spectral range all belong to the isotropic Bi^{4+}_{Ge} defect with the hole highly delocalized onto the four surrounding oxygen atoms. Similar measurements have also been performed on BTO, BSO and BGO doped with several transition metal ions [20]. We have proposed a simple model which explains all the results presented in this paper, without any sophisticated calculation. Some apparent discrepancies with early ODMR results on sillenite crystals have been noted and we have made it clear that the scanning rate or else the power or the field dependence of the two relaxation times plays an important role. More detailed considerations on rate equations along, e.g., the lines of [21] should await the stimulus of additional kinetics measurements under different, well defined, conditions.

A detailed understanding of the absorption and MCD features is still lacking and one can speculate whether they are due to a $^2A_1 \rightarrow {}^2T_2$ internal transition or to a charge transfer transition with the hole being expelled to the valence band to produce Bi^{3+} or an electron being promoted to the conduction band to produce Bi^{5+}. Neither of the two last proposals can in principle be excluded since, although electron photoconductivity is

probably dominant, hole photoconductivity has also been occasionally reported [22, 23].

Acknowledgments

One of us (N Romanov) is grateful to the ESPCI and the city of Paris for the award of a research fellowship in 1994. We are indebted to the French CNRS (UPR A0005) and the Deutsche Forschungsgemeinschaft (SFB225/C4) for financial support. Finally, the Paris group is greatly indebted to its colleagues, H J von Bardeleben, J Monge, D Morisseau and C Alquié for the loan of microwave equipment and useful advice.

References

[1] Arizmendi L, Cabrera J M and Agulló López F 1992 *Int. J. Optoelectron.* 7 149
[2] Hou S L, Lauer R B and Aldrich R E 1973 *J. Appl. Phys.* **44** 2652
[3] Gusev V A, Detinenko V A and Sokolov A P 1983 *Autom. Monit. Meas.* 35
[4] Oberschmid R 1985 *Phys. Status Solidi* a **89** 263
[5] Ennouri A, Tapiero M, Vola J P, Zielinger J P, Moisan J Y and Launay J C 1993 *J. Appl. Phys.* **74** 2180
[6] Briat B, Laulan C, Launay J C and Badoz J 1990 *Tech. Digest Topical Meeting on Photorefractive Materials, Effects and Devices (Aussois 1990)* p 114
[7] Briat B, Laulan Boudy C and Launay J C 1991 *Proc. 7th Eur. Meeting on Ferroelectricity (Dijon, 1991)*; 1992 *Ferroelectrics* **125** 467
[8] Briat B, Fabre J C and Topa V 1993 *Proc. Int. Conf. on Defects in Insulating Materials (Nordkirchen, 1992)* ed O Kanert and J M Spaeth (Singapore: World Scientific) p 1160
[9] Briat B 1993 *Topical Meeting on Photorefractive Materials, Effects and Devices (Kiev, 1993)*
[10] Hamri A, Secu M, Topa V and Briat B 1995 *Opt. Mater.* 4 197
[11] Martin J J, Foldvari I and Hunt C A 1991 *J. Appl. Phys.* **70** 7554
[12] Reyher H J, Hellwig U and Thieman O 1993 *Phys. Rev.* B **47** 5638
[13] Hellwig U, Thiemann O, Reyher H J and Romanov N G 1993 *Proc. Int. Conf. on Defects in Insulating Materials (Nordkirchen, 1992)* ed O Kanert and J M Spaeth (Singapore: World Scientific) p 1118
[14] Moya E, Zaldo C, Briat B, Topa V and Lopez F J 1993 *J. Phys. Chem. Sol.* **54** 809
[15] Reyher H J, Schulz R and Thiemann O 1994 *Phys. Rev.* B **50** 3609
[16] Spaeth J M and Lohse F 1990 *J. Phys. Chem. Sol.* **51** 861
[17] Grabmaier B C and Oberschmid R 1986 *Phys. Status Solidi* a **96** 199
[18] Stephens P J 1976 *Advances in Chemical Physics* vol 35, ed I Prigogine and S A Rice (New York: Wiley) p 197
[19] Kunzer M, Jost W, Kaufmann U, Hobgood H M and Thomas R N 1993 *Phys. Rev.* B **48** 4437
[20] Briat B, Hamri A, Reyher H J, Ramaz F, Launay J C and Gospodinov M 1995 *Topical Meeting on Photorefractive Materials, Effects and Devices (Estes Park, CO, 1995)*
[21] Koschnick F K, Rac M, Spaeth J M and Eachus R S 1993 *J. Phys.: Condens. Matter* 5 733
[22] Pauliat G, Allain M, Launay J C and Roosen G 1987 *Opt. Commun.* **61** 321
[23] Strohkendl F P and Hellwarth R W 1987 *J. Appl. Phys.* **62** 2450